

Transformation of the Normal Distribution for Monte Carlo modeling of regions of Adult trabecular bones for use in Computational Models of Exposure

José Wilson VIEIRA^{1,2}, Viriato LEAL NETO^{1,3}, José de Melo LIMA FILHO^{1,3} e Fernando Roberto de Andrade LIMA^{3,4}

¹ Instituto Federal de Educação, Ciência e Tecnologia de Pernambuco

Av. Prof. Luís Freire, 500
CEP 50740-540 Recife, PE

² Escola Politécnica de Pernambuco - Universidade de Pernambuco

Rua Benfica, 455
CEP 50750-470 Recife, PE

³ Departamento de Energia Nuclear – Universidade Federal de Pernambuco

Av. Prof. Luís Freire, 1000
CEP 50740-540 Recife, PE

⁴ Centro Regional de Ciências Nucleares do Nordeste – Comissão Nacional de Energia Nuclear

Av. Prof. Luís Freire, 200
CEP 50740-540 Recife, PE

ABSTRACT

One of the biggest challenges in numerical dosimetry is to estimate the absorbed dose by the radiosensitive soft tissue of the skeletal inside the cavities of trabecular bone. These tissues are formed by hematopoietic cells of RBM (Red Bone Marrow) and osteogenic cells located on the endosteal surfaces of trabecular bone, called BSC (Bone Surface Cells). The greatest difficulty in evaluating of the absorbed dose in RBM and BSC is to represent realistically the structure of trabecular bone. Since 2006, members of the Research Group on Numerical Dosimetry (GDN/CNPq) publish papers on this subject. The bone dosimetry presented so far is based on the transport of radiation through voxels of trabecular bone obtained from real micro-CT images of five parts of the adult skeleton: skull, spine, rib/sternum, pelvis and femur. One of the difficulties it has observed is the obtaining of these real images, which involves appropriate acquisition machines and ethical questions that could be avoided if the images were virtual. Another difficulty is of computational nature: the *trabeculae* of human bones have linear dimensions of about 0.1 mm while the finest anthropomorphic simulators used in dosimetric evaluations are typically made up of cubic voxels with edge of about 1 mm. Thus, a voxel of these phantoms corresponds to a cube of 1000 voxels in the micro-CT images! This work presents a Monte Carlo method to obtain synthetic images of regions of trabecular bone in adults. The method is based on the standard Gaussian probability density function (pdf), modified by a transformation that moves its maximum over its domain, it changes its intensity and the width of the curve. Using a programming language that provides a good uniform random number generator, it can implement a transformation method of uniform pdf in normal pdf (for example, the Box-Muller method) and then transform normal samples as normal translated. In this work, these steps were implemented to obtain and analyze curves of the count of clusters (set of bone voxels) along the three dimensions of a volume generated on the computer as function of the size of these. Adjusting these charts served as the basis for obtaining the virtual bone samples in appropriate

dimensions. So, when the program ends, the sample for a given bone is ready to be transformed into text file that is used as input in the exposure computer models used by the GDN. This was done for the EGSnrc/MSTA model where MSTA is the acronym for the adult male voxel phantom in the standing position of the Department of Nuclear Energy, Federal University of Pernambuco. The results for internal sources are presented and discussed in this paper. Adjustments in the method are in progress, but the dosimetric results are already promising.

Keywords: Dosimetry, Computational Models of Exposure, EGSnrc Code, Voxel Phantom, Normal Distribution.

1.INTRODUCTION

One of the biggest challenges in numerical dosimetry is to estimate the dose of ionizing radiation absorbed by the soft tissues of the skeleton into the cavities of the trabecular bone. The radiosensitive soft tissues of skeleton are formed by the hematopoietic cells of RBM and by osteogenic cells located at endosteal surface of trabecular bone, the BSC. The greatest difficulty in evaluating the absorbed dose by RBM and BSC consists in represent of realistic form the complex structure of trabecular bone. For illustration, Figure 1 shows the distribution of bone trabeculae of a stack of micro-CT images of a human lumbar vertebra (Kramer et al. 2009). This and all 3D images presented in this paper were obtained with “Fiji” free software, available at <http://fiji.sc/wiki/index.php/Downloads>.

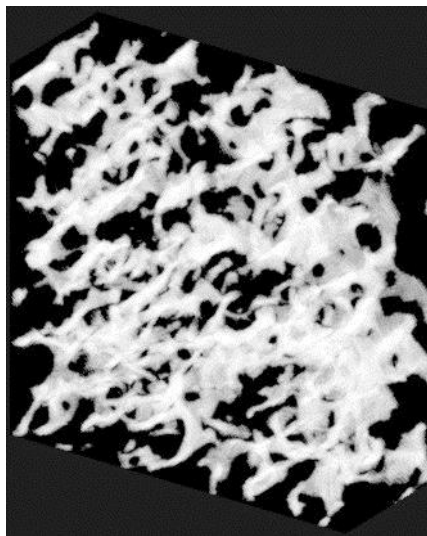


Figure 1: 3D view of the distribution of trabecular bone sample of a lumbar vertebra.

Samples like these are used in current exposure computational models of exposure (ECMs) developed by the GDN / CNPq (<http://dosimetrianumerica.org>). These ECMs are based on voxel phantoms and Monte Carlo code EGSnrc. To estimate the energy deposited in the BSC and RBM of a phantom, the GDN / CNPq has used a method based on micro-CT images developed by Kramer et al. (2009). This method requires samples of five groups of trabecular bones, ribs (including the clavicles and sternum), spine, long bones, pelvis and skull. The samples used for the current ECMs by GDN / CNPq are adults and have been provided by other research institutes. Here is the greatest difficulty in reproducing the method of micro-CT for bone dosimetry: beyond the necessity of bone images of real people with a resolution of micrometers, the distribution of bone marrow in the human body, according to International Commission on Radiological Protection (ICRP 70, 1995) varies greatly with age.

This paper proposes the replacement in ECMS of real micro-CT images for synthesized images on the computer. The synthetic images presented here were produced by Monte Carlo techniques based on three pdfs: a uniform, regular and modified normal (Johnson 1949). To produce the images were developed some programs in C # (Sharp 2010) based on *System.Random.NextDouble()* algorithm, true random number generator, uniformly distributed in the interval [0, 1). In general, using the class *CFantoma* (Vieira and Lima 2009), is initially defined a parallelepiped of 0's. Based on information on the bone to be modeled, a percentage of 0 are replaced by 255. The ways in which exchange occurs between identifiers (ids) 0 and 255 characterize the methodological essence of this article. After a *CFantoma* object is saved as a binary file that allows construction of 3D images as shown in Figure 1. This type of file, called IGS (Interactive Graphic Simulations) by GDN / CNPq, is transformed into text files used in the ECMS as samples of trabecular bone.

The results of the dosimetric evaluation using synthetic images were compared with similar results obtained with the traditional ECMS. For the purpose proposed here, the Monte Carlo methods used were effective in producing substitute images of real bones micro-CT.

2.MATERIALS AND METHODS

Some of the steps necessary to construct 3D images on the computer requested the development of some computer programs. This was done in the integrated development environment of Microsoft Visual Studio 2010 as project *WPF Application* (Xu 2009), which uses the C # language in an environment of code and markup language *XAML* (eXtensible Application Markup Language) in a design environment.

The steps for construction of 3D images consisted in the selection of Monte Carlo algorithms (random number generators (RNGs)) for sample of the five bone regions, test and choose the parameters of the RNGs and implementation of Monte Carlo techniques to obtain 3D images.

As a final step, dosimetric evaluations were performed with ECM *MSTA / EGSnrc* (Cassola 2011), containing micro-CT real images and also with the new images produced in this work.

Following each of these steps is shown in more detail.

2.1. CONSTRUCTION OF 3D IMAGES

As seen in Figure 1, the 3D images of trabecular bones are binary in the sense that it only takes two ids to fill the 3D collection that represent themselves in the program code: one for the bone and the other for the soft tissue that fills the "caves". When one wishes to view the image, at which the contrast must be emphasized, one can use 0 and 255, in situations of calculations, as in the dosimetric evaluation, 1 and 2. Any other two numbers between 0 and 255 may be used.

To define the internal 3D collection corresponding to the desired trabecular bone block, was used the class *CFantoma*, developed for editing voxel phantoms. Therefore, step 0 for the construction of 3D images consisted in to define a *CFantoma* object and initialize its element with 0.

2.2. Monte Carlo Techniques for Transformation of PDF Uniform

Play a 3D image as shown in Figure 1 from algorithms requires studies on the nature of the image and methods that coded the information obtained.

It is known that the images are binary and there is a class that can start one of these images with the dimensions given by the user and with the elements set to 0. Now, computational methods are needed to turn this 3D matrix of 0's in a collection of values 0 and 255 with attributes that result in some similarity with the actual bone samples available.

The GDN / CNPq has conducted some tests in search of these transformers methods (Lima Filho et al. 2011). In this work, the research was focused on Monte Carlo techniques that transform a uniform pdf to one pdf where a maximum occurs in your domain (Kalos and Whitlock 1986; Duffy and Kienitz 2009). This is because, as shown in Figure 1, the distribution of sets of voxels (clusters) of the bone along any of the three dimensions of the sample is not uniform.

To obtain a real RNG, uniformly distributed in the interval [0, 1] in the Visual Studio environmental just declare an object of type *System.Random*:

```
private Random rnd;
```

and initialize it in the class constructor of the program:

```
this.rnd = new Random();
```

In an event function, the samples are generated in a loop and stored in a generic list for real numbers:

```
for (i = 0; i < this.NAmostras; i++)
    this.listDoubleAmostras.Add(this.rnd.NextDouble());
```

Figure 2a shows a test of the subintervals to RNG accessed by *rnd.NextDouble*. To perform this test were generated 10^7 samples generated and counted the occurrences in 100 equally spaced intervals between 0 and 1. It can be considered that RNG passed this test without problems since the count in each of the 100 intervals was approximately 10^5 . Of course, more robust statistical tests (Vieira 2001) help in the validation of the algorithms implemented in programming languages.

The standard one-dimensional normal (or Gaussian) pdf (Kalos and Whitlock 1986) is defined as

$$f(z) = \frac{1}{\sqrt{2\pi}} e^{-\frac{1}{2}z^2}, \quad -\infty < z < \infty. \quad (1)$$

Now, to create a list of *NAmostras* z of Eq. (1) was used the loop

```
for (i = 0; i < this.NAmostras; i++)
    this.listDoubleAmostras.Add(CGNA.rann(media, sigma));
```

where “media” is the average ($z = 0$) and “sigma” is the standard deviation of the distribution ($\sigma = 1$). The “ran” function is defined in a C # class *CGNA*. Here's the code:

```
private static double y2_boxMuller;
private static int use_last = 0;
public static double rann(double MEDIA, double SIGMA)
{
    double x1, x2, w, y1_boxMuller, gauss;
    if (use_last != 0)
    {
        y1_boxMuller = y2_boxMuller;
        use_last = 0;
    }
    else
    {
        do
```

```

    {
        x1 = 2.0 * ranu() - 1.0; //Método Box-Muller polar
        x2 = 2.0 * ranu() - 1.0;
        w = x1 * x1 + x2 * x2;
    } while (w >= 1.0);
    w = Math.Sqrt((-2.0 * Math.Log(w)) / w);
    y1_boxMuller = x1 * w;
    y2_boxMuller = x2 * w;
    use_last = 1;
}

if (SIGMA != 0)
    gauss = SIGMA * y1_boxMuller + MEDIA;
else
{
    MessageBox.Show("Problemas com o GNA rann()! SIGMA = 0");
    gauss = double.MinValue;
}

return gauss;
}

```

This is polar implementation to the box-muller method (Box Muller and 1958; Kalos and Whitlock 1986).

Figure 2b shows the test for *CGNA.rann* (0, 1) subintervals. To perform this test were also generated 10^7 samples and counted the occurrences in 100 equally spaced intervals between -5σ and 5σ .

Similarly to the uniform pdf have been disposed only with visual arguments based on the image of Figure 1, one can be again argued that the clusters distributions along the three directions of the trabecular bone block does not have a central distribution as symmetrical as Gaussian. It is more reasonable to investigate distributions that have a maximum as the Gaussian, but with control parameters for the position of this maximum along the domain.

Johnson (1949) shows that the pdf obtained by modification of normal one

$$p(y) = \frac{\delta}{\sqrt{2\pi}} \frac{1}{y(1-y)} e^{-\frac{1}{2} \left[\gamma + \delta \ln \left(\frac{y}{1-y} \right) \right]^2}, \quad 0 < y < 1, \quad (2)$$

may be sampled by the algorithm

$$y = \frac{1}{1 + e^{\frac{(z-\gamma)}{\delta}}}, \quad (3)$$

where z is one standard normal random variable, and γ (real) and δ (real positive) are parameters which control the shape of the curve $p(y)$ over its domain.

To create a list of *NAmostras* y from the Eq. (3), was used to loop

```

for(i = 0; i < this.NAmostras; i++)
    this.listDoubleAmostras.Add(CGNA.rannt(this.delta, this.gama));

```

where the function *rannt* is defined according to Eq. (3), by:

```

public static double rannt(double delta, double gama)
{
    double normal = rann(0, 1);

```

```

return 1 / (1 + Math.Exp(-(normal - gama) / delta));
}

```

Figures 2c, 2d, 2e and 2f show the utility of the parameters γ and δ . Two *DecimalUpDown* type controls (this control is part of the *Extended WPF Toolkit 1.5.0*, available at <http://wpftoolkit.codeplex.com/releases/view/71499>) were used to change their values γ and δ . Figures 2c and 2d, $\delta = 1$. When $\gamma > 0$, the maximum of the pdf (2) approaches $y = 0$, where $\gamma < 0$, the maximum approaches $y = 1$, when $\gamma = 0$, the function has a maximum centered. Therefore the parameter γ shifts the maximum of the function over its domain.

Figures 2e and 2f, $\gamma = 1$. The graphs of these figures one can see that δ concentrates the samples tending to an exponential pdf ($0 < \delta < 1$) or a normal ($\delta > 1$).

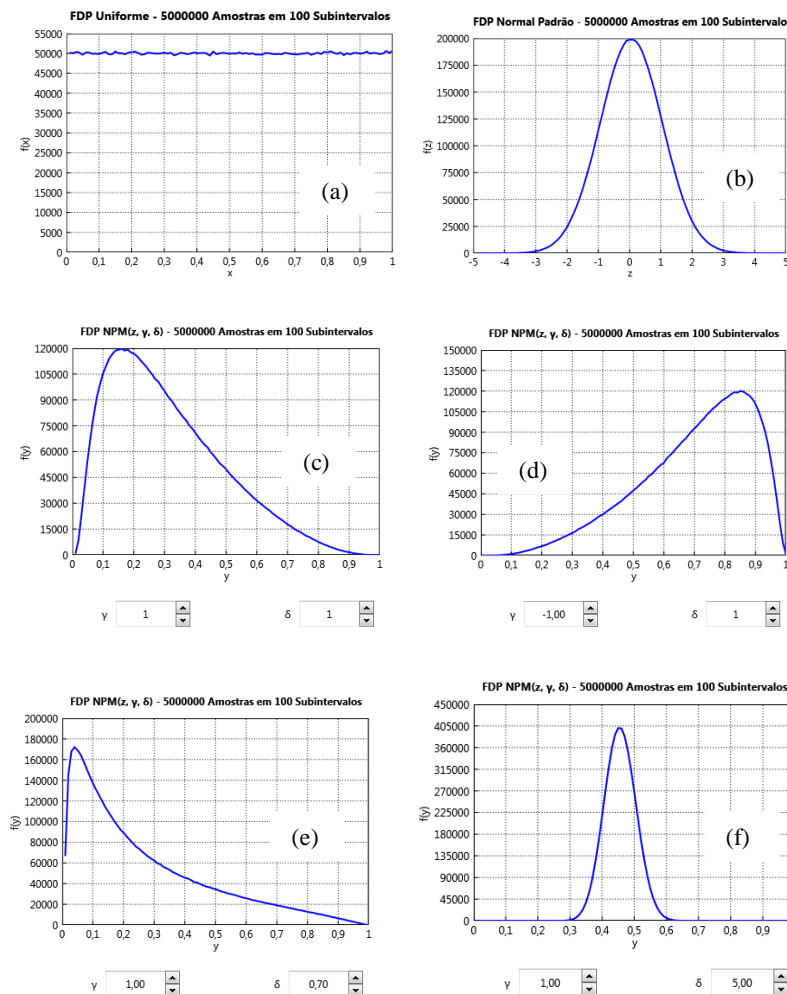


Figure 2: Testing for the pdf of the subintervals (a) $U(0, 1)$; (b) $N(0, 1)$; (c) to (f) $NPM(z, \gamma, \delta)$.

These features of the pdf (2) were used to model a pdf that describes distributions of clusters of voxels along the three dimensions of trabecular bone samples.

2.3. Testing and Choice of Parameters

To get an idea of how to model the pdfs required for the sampling of clusters of bone voxels to be distributed in a block so as similar as possible to the distributions of voxels in real bones,

were further developed code in C # and / or XAML CFantoma to read an object, get three generic lists with the percentage of occurrences depending on the size of the clusters, one for each dimension of the phantom input, and display charts of this data.

These steps have been implemented and Figure 3 shows graphs of the percentage of occurrence versus the cluster size for the same sample of Figure 1.

On the basis of Figures 1, 2 and 3, it can be stated that the profiles of the distribution along the three dimensions of the sample used in this example may be represented by pdf (2), expanding appropriately its domain and adjusting the values of parameters γ and δ . The other samples available in this study have similar behaviors.

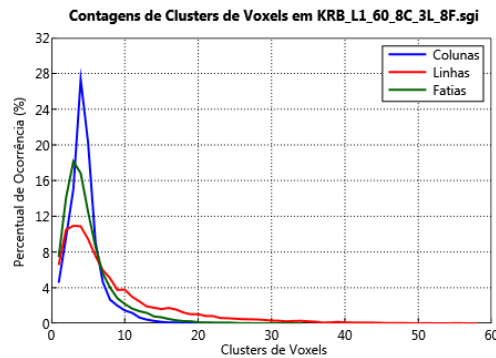


Figure 3: Distribution of clusters of voxels in the three dimensions of a sample of human lumbar vertebra.

For the graphs shown in the top of Figure 4, codes have been developed to repeat the graph of Figure 3, now in separate windows, and to plot on the same a pdf (2), with equal domain and maximum. Manipulating γ , δ and the mean relative error between the percentage of occurrences of sizes of voxel clusters in real bone and Monte Carlo simulation was possible to adjust the curves of pdf.

Figure 5 shows graphs of the percentage of occurrence versus number of voxel clusters for the sample of the human spine obtained with the data shown in Figure 4, plotted together with similar graphs of real samples (Figure 3). All blocks obtained in this study have dimensions (in pixels) 160 x 60 x 160. As the voxels of the MASH phantom has edge of 1.2 mm and the micro-CT images of 60 μm , the blocks comprise 8 x 8 x 3 voxels of the phantom. The profiles of synthetic images reflect the algorithm (3), but also further processing applied to the images to delete or add voxels in gaps of the volume.

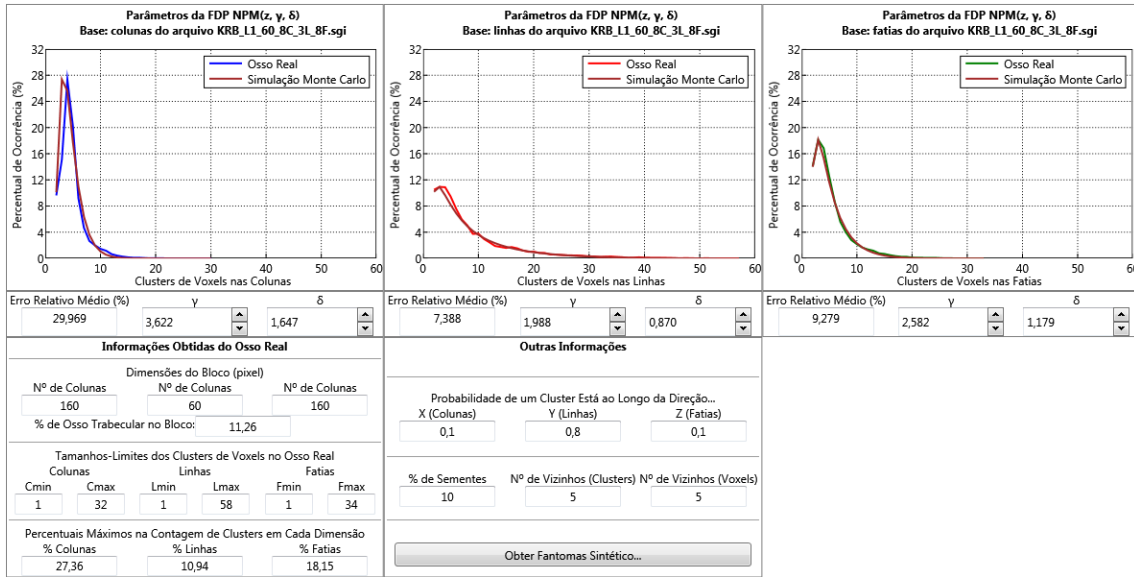


Figure 4: Obtaining the parameters for the algorithm of pdfs NPM (z, γ, δ) used in the construction of the human spine sample.

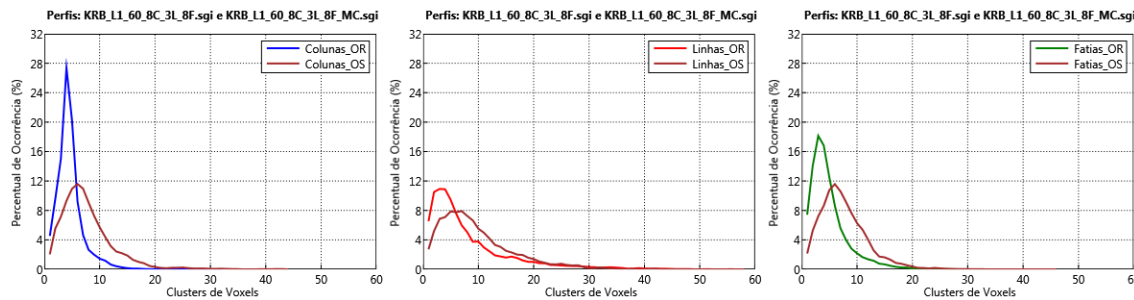


Figure 5: Percentage of occurrence of cluster sizes of trabecular bone due to the number of clusters along the three directions for the bone real sample (OR) and synthetically obtained by the Monte Carlo methods (OS).

With this promising sampling method implemented, was possible obtain virtual samples from five regions of trabecular bones used in computational models of exposure of GDN / CNPq.

2.4. Construction of 3D Synthetic Images

Figure 4 shows the data needed to generate a block for a given trabecular bone. Here are the steps needed to obtain the 3D image of the sample of synthetic human spine shown in Figure 6:

- Get input data shown in Figure 4 and store them in the appropriate internal variables.
- Create phantom bone block with dimensions corresponding to values reported more walls that at the end of the algorithm are eliminated. This avoids the edges.
- Fill the phantom block with 0's and initialize with 0 a counter voxels added.
- To replace 0 by 255 on the block with the amount reported the code ...
 - draws a direction to position the current cluster based on probabilities reported for each direction and in *nextDouble()* uniform RNG;
 - draws to a cluster size based on the algorithm (3) and the lower and upper bounds for the abscissa drawn toward;

- draws to, uniformly, a percentage of voxels of the phantom with 0 to locate the cluster drawn or part of it; the rest of the initial voxels of the clusters are also drawn uniformly required, but with the conditional of having a given number of neighbors of the same species;
- starting from location and direction chosen at randomly, places in the phantom the drawn cluster or part of it. The cluster is added to the phantom independently of there are other voxels in space it will occupy. The counter is incremented by one voxel. If the total amount of voxels drawn is reached, the phantom of the requested block of bone is built. Otherwise, this step is repeated.

Essentially, these steps are implemented for the construction of synthetic 3D images. Additional tasks such as the use of techniques to erase isolated voxels and readjust the percentage of required voxels bone were performed with software already developed by the GDN / CNPq (Vieira et al. 2005; Vieira and Lima 2009).

Figure 6 shows the 3D image of the synthetic spine sample, obtained using the above algorithm. It has the same percentage of bone shown in Figure 1 and its trabecular aspect plays some similarities as the tendency of larger clusters are arranged in the y direction (the lower thickness in the figure).

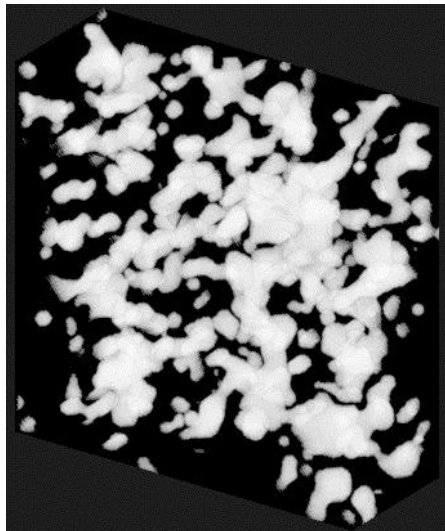


Figure 6: Synthetic 3D image of the spine sample obtained from the data in Figure 4.

2.5. DOSIMETRIC EVALUATIONS

The samples for the five bones were obtained, its files IGS were transformed into text files and exchanged for similar real bones contained in the ECM MSTA / EGSnrc results are presented in sequence.

3.RESULTS AND DISCUSSION

Table 1 shows the input parameters for the algorithm (3).

Table 1: Parameters used in the normal pdf modified to generate the synthetic samples of trabecular bone.

Bone Region	Columns		Lines		Slices	
	γ	Δ	γ	δ	γ	δ
Ribs (sternum)	2,977	0,975	3,067	1,670	3,654	0,936
Spine	3,581	1,626	1,9680	0,870	2,490	1,114
Long bones (femur)	2,932	1,239	3,098	1,250	2,210	1,090
Pelvis	2,914	1,140	2,847	1,137	2,636	1,026
Skull	3,050	0,873	2,099	0,831	3,186	0,949

Table 2 shows that the percentage of voxels of trabecular bone in real samples sets (OR) and synthetic (OS) are practically the same.

Table 2: Five bone regions with the percentage of trabecular bone provided by ICRP 70 (2nd column) and the synthetic images obtained with this work.

Bone Region	% of bone - ICRP	% of bone of synthetic images
Ribs (sternum)	11,44	11,45
Spine	11,25	11,26
Long bones (femur)	15,24	15,24
Pelvis	21,15	21,17
Skull	51,56	51,42

Figure 7 shows 3D images of five real bones samples (the first row of images) and synthetic. Only in a visual analysis one may indicate that the synthetic samples for long bones, pelvis and skull are more like their real versions.

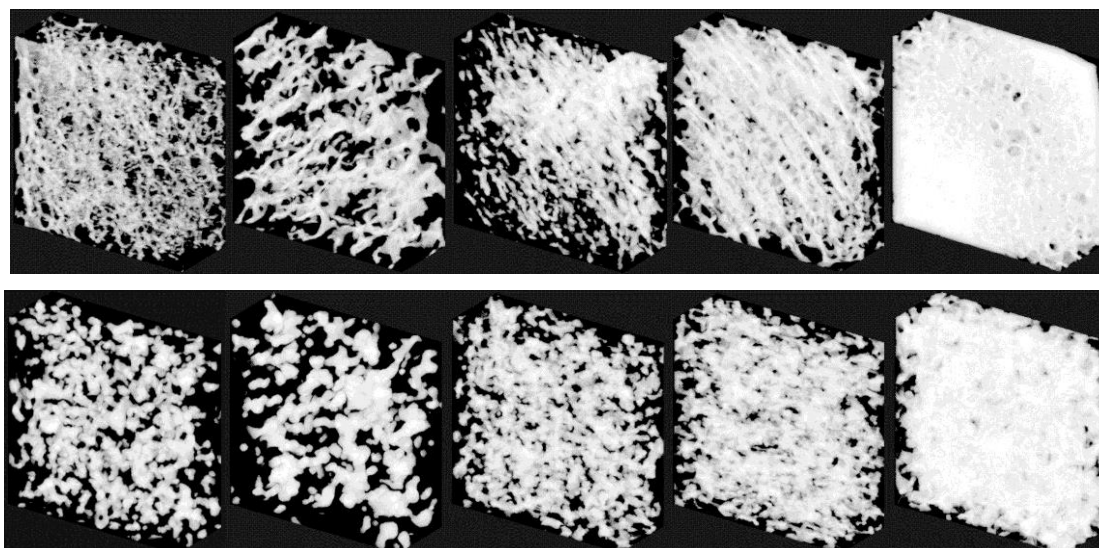


Figure 7: 3D images of real trabecular bone samples (first line) and synthetic used in the ECM MSTA / EGSnrc.

Table 3 shows dosimetric results using the two sets of available samples: those obtained from real bones and those produced on the computer. In the simulation we used the ECM MSTA / EGSnrc with photons with energies ranging from 10 to 4000 keV and enough stories (5.00 E +07) to obtain the coefficients of variance shown in the table. The organ-source chosen was the

testes and the conversion factor was absorbed fractions (AF). The table shows values of AFs for tissues-target RBM and BSC of the pelvis.

Table 3: Dosimetric results using dosimetric sets of real trabecular bone samples (OR) and synthesized on the computer (OS). Organs-source: testes; tissues-target: RBM and BSC of the pelvis.

Photon Energy (keV)	RBM					BSC				
	MSTA OR		MSTA OS		OR/OS	MSTA OR		MSTA OS		OR/OS
	AF	Erro (%)	AF	Erro (%)		AF	Erro (%)	AF	Erro (%)	
10	0,00E+00	0,00	0,00E+00	0,00	1,000	0,00E+00	0,00	0,00E+00	0,00	1,000
15	1,85E-07	32,35	2,78E-07	26,35	0,663	6,49E-08	53,90	8,39E-08	47,72	0,773
20	2,04E-05	3,03	2,12E-05	2,96	0,959	8,25E-06	4,65	8,03E-06	4,66	1,027
30	3,01E-04	0,75	3,04E-04	0,74	0,990	1,20E-04	1,13	1,35E-04	1,07	0,888
50	7,99E-04	0,38	8,07E-04	0,38	0,990	3,85E-04	0,54	4,19E-04	0,52	0,919
60	9,07E-04	0,33	9,16E-04	0,33	0,991	4,49E-04	0,47	4,89E-04	0,44	0,917
70	9,70E-04	0,29	9,77E-04	0,29	0,993	4,78E-04	0,42	5,20E-04	0,40	0,918
80	1,01E-03	0,27	1,01E-03	0,26	0,995	4,94E-04	0,39	5,39E-04	0,37	0,917
100	1,05E-03	0,23	1,06E-03	0,23	0,991	4,94E-04	0,35	5,41E-04	0,33	0,913
200	1,11E-03	0,19	1,11E-03	0,19	0,998	4,54E-04	0,29	4,96E-04	0,28	0,915
500	1,14E-03	0,18	1,14E-03	0,18	0,996	4,31E-04	0,24	4,71E-04	0,23	0,916
1000	1,11E-03	0,18	1,11E-03	0,18	1,000	4,10E-04	0,21	4,49E-04	0,21	0,913
1500	1,05E-03	0,19	1,05E-03	0,19	1,001	3,88E-04	0,20	4,26E-04	0,20	0,912
2000	1,01E-03	0,20	1,00E-03	0,20	1,002	3,70E-04	0,20	4,05E-04	0,20	0,914
4000	8,69E-04	0,21	8,65E-04	0,21	1,004	3,19E-04	0,21	3,48E-04	0,21	0,915
Média					0,972					0,917

Table 4 shows the number of voxels for the BSC of the various bone tissue. The reasons for OR / OS confirm that show the 3D images of Figure 7: Samples with lower percentages of trabecular bone (ribs and spine) have ratios greater than unity.

Table 4: Voxel quantities (real and synthetic) of segmented bone tissue in the phantom MASH.

TISSUE	OR	OS	OR / OS
CRANIUM BSC	23905	24770	0,965
MANDIBLE BSC	2512	2598	0,967
CERVICAL SPINE BSC	6638	5515	1,204
THORARCIC SPINE BSC	19588	16005	1,224
LUMBAR SPINE/SACRUM BSC	24826	20304	1,223
PELVIS BSC	35832	39351	0,911
RIBS BSC	23687	17605	1,345
STERNUM BSC	4050	2864	1,414
RIGHT CLAVICLE BSC	1189	867	1,371
LEFT CLAVICLE BSC	1193	872	1,368
RIGHT SCAPULA BSC	3917	2898	1,352
LEFT SCAPULA BSC	3912	2902	1,348
RIGHT UPPER ARM BSC+MED BS	3267	3370	0,969
LEFT UPPER ARM BSC+MED BSC	3286	3365	0,977
RIGHT LOWER ARM BSC+MED BS	9304	9599	0,969
LEFT LOWER ARM BSC+MED BSC	9322	9594	0,972
RIGHT UPPER LEG BSC+MED BS	12241	12606	0,971
LEFT UPPER LEG BSC+MED BSC	12247	12612	0,971
RIGHT LOWER LEG BSC+MED BS	26397	27185	0,971
LEFT LOWER LEG BSC+MED BSC	26394	27172	0,971
BONE SURFACE CELLS+MED BSC	253707	242054	1,048

4.CONCLUSIONS AND PERSPECTIVES

Results of this study are preliminary, but promising. The main algorithm presented here to generate samples of bone voxels was efficient as seen in 3D images of Figure 7. Adjustments in the used pdf control parameters as well as in the controls to add or erase new voxels, will make more efficient the process as a whole, i.e., the generation of 3D synthetic images.

Continuing research will result in a doctoral thesis already in progress.

ACKNOWLEDGEMENT: CNPq

REFERENCES

BOX, G. E. P. and MULLER, M. E., **A Note on the Generation of Random Normal Deviates**, Technical Report N° 13, Statistical Techniques Research Group, Department of Mathematics, Princeton University, 1958.

CASSOLA V. F., **Desenvolvimento de Fantomas Humanos Computacionais Usando Malhas Poligonais em Função da Postura, Massa e Altura**, Tese Doutorado em Tecnologias Energéticas Nucleares, Universidade Federal de Pernambuco, UFPE, Brasil, 2011.

DUFFY, D. J. and KIENITZ, J., **Monte Carlo Frameworks: Building Customizable High-performance C++ Applications**, John Wiley & Sons, Great Britain, 2009.

ICRP 70, **Basic Anatomical and Physiological Data for Use in Radiological Protection: The Skeleton**, International Commission on Radiological Protection, Pergamon Press, Oxford, 1995.

JOHNSON, N. L., **Systems of Frequency Curves Generated by Methods of Translation**, *Biometrika*, vol. 36, No. 1/2, 149-176, 1949.

KALOS, M. H. and WHITLOCK, P. A., **Monte Carlo Methods**, A Wiley-Interscience Publication, New York, 1986.

KRAMER, R., KHOURY, H. J., Vieira, J. W., Robson Brown, K. A., **Skeletal Dosimetry for External Exposures to Photons Based on μ CT Images of Spongiosa: Consideration of Voxel Resolution, Cluster Size, and Medullary Bone Surfaces**, *Medical Physics*, vol. 36 (11), 5007-5016, 2009.

LIMA FILHO, J. M., VIEIRA, J. W., LIMA, V. J. M., LIMA, L. F., LIMA, F. R. A., VASCONCELOS, W. E., **Bone Dosimetry Using Synthetic Images to Represent Trabecular Bones of Five Regions of the Human Body**, *poster*. INAC 2011 (International Nuclear Atlantic Conference), Belo Horizonte, MG, Brasil, October 24-28, 2011.

SHARP, J., **Microsoft Visual C#2010 Step by Step**, Microsoft Press, Redmond, Washington, 2010.

VIEIRA, J. W., **Uso de Técnicas Monte Carlo para Determinação de Curvas de Isodose em Braquiterapia**, Dissertação Mestrado em Tecnologias Energéticas Nucleares, Universidade Federal de Pernambuco, UFPE, Brasil, 2001.

VIEIRA, J. W., Stosic, B., Lima, F. R. A., Kramer, R., Santos, A. M. e Lima, V. J. M., **Um Software para Editar Fantomas de Voxels e Calcular Coeficientes de Conversão para a Proteção Radiológica**, Primeiro Congresso Brasileiro de Proteção Radiológica, Rio de Janeiro, 02 a 05 de novembro de 2005.

VIEIRA, J. W. and LIMA, F. R. A., **A Software to Digital Image Processing to be Used in the Voxel Phantom Development**, *Cellular and Molecular Biology*, V.55, p. 16-22, 2009.

XU, J., **Practical WPF Charts and Graphics**, APRESS Copyrighted Material, USA, 2009.